

## Modeling the Inhibitory Effects of Octylphenol Polyethoxylates on *Aeromonas* sp. Growth: Evaluating Bioremediation Kinetics through Advanced Growth Models

Umar Abubakar Mohamad<sup>1</sup>, Normala Halimoon<sup>2</sup>, Wan Lutfi Wan Johari<sup>2</sup>, Garba Uba<sup>3</sup> and Ibrahim Sabo<sup>4\*</sup>

<sup>1</sup>Department of Biological Sciences, Faculty of Science, Gombe State University, P.M.B 127, Tudun Wada, Gombe, Gombe State, Nigeria.

<sup>2</sup>Department of Environment, Faculty of Forestry and Environment, Universiti Putra Malaysia, 43400 Serdang, Selangor, Malaysia.

<sup>3</sup>Department of Science Laboratory Technology, College of Science and Technology, Jigawa State Polytechnic, Dutse, PMB 7040, Nigeria.

<sup>4</sup>Department of Microbiology, Faculty of Pure and Applied Sciences, Federal University Wukari, P.M.B. 1020 Wukari, Taraba State, Nigeria.

\*Corresponding author:

Ibrahim Alhaji Sabo

Department of Microbiology,

Faculty of Pure and Applied Sciences,

Federal University Wukari,

P.M.B. 1020 Wukari,

Taraba State,

Nigeria.

Email: [ibrahimsabodzk@dzk.com](mailto:ibrahimsabodzk@dzk.com)

### HISTORY

Received: 25<sup>th</sup> Oct 2023  
Received in revised form: 24<sup>th</sup> Nov 2024  
Accepted: 27<sup>th</sup> Dec 2023

### KEYWORDS

*Nigella sativa*  
*Ziziphus jujuba*  
Medicinal plant  
Peptic ulcer  
Nutrients

### ABSTRACT

Octylphenol polyethoxylates (OPEs) constitute a class of non-ionic surfactants extensively employed in various industrial applications. However, concerns have arisen regarding the potential environmental and human health impacts of OPEs because of their widespread use and persistence in aquatic environments. Bioremediation of OPE in the environment using OPE-degrading bacterium is appealing as bacterial metabolism converts OPE to harmless carbon dioxide and water as byproducts. In this study, various secondary growth models such as Luong, Yano, Teissier-Edward, Aiba, Haldane, Monod, Han, and Levenspiel were employed to model the inhibitory effect of high OPE concentrations to the growth rate of *Aeromonas* sp. TXBc10 the bacterium on OPE. Following thorough statistical analyses such as root-mean-square error (RMSE), adjusted coefficient of determination ( $\text{adj}R^2$ ), bias factor (BF), and accuracy factor (AF), the Teissier model emerged as the most optimal choice. All of the studied models showed good fittings except Moser, Monod and Hinshelwood which showed the poorest curve fitting. The calculated value for the Luong's constants maximal degradation rate, half saturation constant for maximal degradation, maximal concentration of substrate tolerated and curve parameter that defines the steepness of the growth rate decline from the maximum rate symbolized by  $q_{\text{max}}$ ,  $K_s$ ,  $S_m$ , and  $n$  were  $8.91 \text{ h}^{-1}$  (95% confidence interval or C.I. from 7.15 to 10.67), 1116.19 mg/L (95% C.I. from 815.53 to 1416.84), 1074.6 mg/L (95% C.I. from 1037.8 to 1111.5) and 11.90 (95% C.I. from 5.30 to 18.51), respectively. It is possible that these new constants found when modeling could be useful inputs for future modeling efforts. In addition incorporating substrate inhibition kinetics into risk assessment models contributes to a more accurate evaluation of the potential risks associated with the presence of toxic substrates in contaminated sites. This information is vital for decision-making in environmental management.

### INTRODUCTION

Due to their surfactant properties, Octylphenol polyethoxylates (OPEs) find applications in various industrial processes. They are utilized for emulsification, creating stable emulsions that aid in mixing substances that would typically separate, such as oil and water, proving valuable in industries like agriculture and

cosmetics. OPEs also serve as effective wetting agents, enhancing the spreading and absorption of liquids on solid surfaces, making them useful in formulating agrochemicals, paints, and coatings. In the textile industry, OPEs function as surfactants for dyeing processes, dispersing dyes evenly and improving their penetration into fibers. Industrial cleaning products benefit from OPEs as their emulsifying and wetting

properties facilitate the removal of dirt and contaminants [1]. Additionally, OPEs are employed in the paper and pulp industry as additives to improve the wetting and penetration of chemicals during pulping and papermaking processes. They play a role in agrochemical formulations, enhancing the distribution and effectiveness of active ingredients on crops. OPEs find application in metalworking fluids, improving lubrication and cooling during machining processes by maintaining stable emulsions in water-based fluids [2]. Personal care products, such as shampoos and lotions, may contain OPEs due to their emulsifying and dispersing properties. In adhesives and sealants, OPEs contribute to improved wetting of surfaces, enhancing overall product performance.

Furthermore, in polymer industries, OPEs may be utilized as emulsifiers in polymerization processes, aiding in the dispersion of polymer particles and stabilizing reactions. It's important to note that despite their widespread past use, concerns about the environmental and health impacts of OPEs have led to regulatory scrutiny. As a result, alternative, more environmentally friendly surfactants are being explored in various industries [3].

OPEs exhibit toxicity towards aquatic organisms like fish, algae, and invertebrates by disrupting cell membranes and affecting normal functioning. Accumulation in sediments and bioaccumulation in aquatic species pose long-term exposure risks, leading to potential ecological consequences [2,4–6]. A major concern is their capacity to function as endocrine disruptors, particularly with documented estrogenic activity that interferes with the endocrine system of aquatic organisms, resulting in reproductive abnormalities and compromised success in exposed organisms. Despite well-documented environmental impacts, research also emphasizes potential human health risks associated with OPE exposure. These compounds can enter the human body through various pathways, raising concerns about their role in hormone regulation and the development of specific health conditions. Environmental monitoring and biomonitoring data, reviewed in a study assessing human exposure to nonylphenol (NP), indicate source-specific Margins of Exposure (MOEs) ranging from 2863 to  $8.4 \times 10^7$ , well above 1000, suggesting reasonable certainty of no harm for both source-specific and aggregate exposures to NP [1]).

In a study by Baldwin et al. [4], it was observed that nonylphenol polyethoxylate (NPPG) at 5.0 mg/liter inhibits testosterone elimination in *Daphnia magna*, mirroring the effects seen with its degradation product 4-nonylphenol. Interestingly, NPPG did not induce significant chronic toxicity, suggesting that environmental concentrations of NPPG may not pose a risk to invertebrates. Another investigation by TenEyck and Markee [5] focused on assessing the toxicity of three phenolic compounds—nonylphenol (NP), nonylphenol monoethoxylate (NP1EO), and nonylphenol diethoxylate (NP2EO)—to *Pimephales promelas* and *Ceriodaphnia dubia*. The study involved testing binary and tertiary mixtures, commonly found in surface waters due to wastewater discharges.

The fathead minnows exhibited LC50 values of 136, 218, and 323  $\mu\text{g/L}$  for NP, NP1EO, and NP2EO, respectively, indicating potential additive or synergistic effects in mixtures. Furthermore, Song and Bielefeldt [6] explored the impact of five alkylphenol polyethoxylate nonionic surfactants on the microbial degradation of glucose and pentachlorophenol (PCP) by *Sphingomonas chlorophenolicum* RA2. The study revealed that surfactants with mid-range hydrophile-lipophile balance (HLB) values (13.5–15) were most compatible with substrate

degradation. Interestingly, the lowest HLB surfactant inhibited RA2 growth, while the highest HLB surfactant showed inhibitory effects only at concentrations well above its critical micelle concentration (CMC). The surfactants exhibited more inhibitory effects on RA2's PCP biodegradation compared to glucose, suggesting potential interactions with membrane-associated PCP-degrading enzymes [6]. These findings have practical implications for selecting surfactants in remedial applications involving biodegradation or oil dispersion. In a previous study, an OPE-degrading bacterium was isolated and characterized as an effort to remediate OPEs. The growth rate of the bacterium on OPE showed significant inhibition at high concentration of OPE

## MATERIALS AND METHODS

### Data acquisition

The graphical data extracted from Figure 4a on the biodegradation of OPE by *Aeromonas* sp. TXBc10 [3], was first converted to degradation rate assuming an incubation period of 120 h and then analyzed using the software tool Webplot digitizer. This software is widely acknowledged and embraced within the scientific community [7], for its capacity to convert scanned figures into digital data. Numerous researchers have consistently recognized its precision and reliability [8,9]. The data was further analyzed and modeled using Curve Expert Professional software (Version 2.6.5) to elucidate the scientific insights and trends within the dataset, contributing to the robustness of the study's findings. This combination of data digitization and advanced software analysis is a common and essential practice in modern scientific research, ensuring the Accuracy and validity of results.

### Fitting of the data

The Marquardt algorithm was employed for nonlinear regression to fit various bacterial growth models (Table 1) and this analysis was conducted using Curve Expert Professional software (Version 2.6.5). The algorithm aims to find the most optimal method for minimizing the sum of squares between predicted and observed values. In this process, the software can be configured manually or automatically to determine the initial parameter values, and the steepest gradient search between the four data points was utilized to estimate the maximum degradation rate ( $q_{max}$ ).

### Statistical analysis

The statistically significant difference between the models was evaluated using various metrics. The following statistical functions were utilized to determine the best models. The RMSE allows number of parameters' penalty and was calculated using Equation 1, where  $n$  illustrates the number of experimental data, where else  $p$  is the number of parameters calculated by the model and experimental data and values predicted by the model are  $Ob_i$  and  $Pd_i$ , respectively [20]. With the regression line approaching the data points, the root mean square error (RMSE) reduces due to the reduced error in the model. More accurate predictions are generated by a model that has a lower error rate.

Comparable in magnitude to the dependent (outcome) variable, the RMSE values span an infinite number of positive infinities. The root mean square error (RMSE) can be employed to assess the extent of imprecision in a statistical model, including regression models. If a value is zero, it signifies that the predicted and actual values are an exact match. The model exhibits superior data fit and generates more precise predictions, as indicated by low RMSE values. In contrast, increased levels indicate a greater magnitude of errors and a reduced number of precise predictions.

**Table 1.** Substrate inhibition mathematical models.

Author	Degradation Rate	Author
Monod	$\frac{q_{max}S}{S + K_s}$	[10]
Haldane	$\frac{q_{max}S}{S + K_s + \left(\frac{S^2}{K_i}\right)}$	[11]
Teissier	$q_{max} \left( 1 - \exp\left(-\frac{S}{K_i}\right) - \exp\left(\frac{S}{K_s}\right) \right)$	[12]
Aiba	$q_{max} \frac{S}{K_s + S} \exp\left(-\frac{S}{K_i}\right)$	[13]
Yano and Koga	$\frac{q_{max}S}{S + K_s + \left(\frac{S^2}{K_i}\right) \left(1 + \frac{S}{K}\right)}$	[14]
Han and Levenspiel	$q_{max} \left( 1 - \left(\frac{S}{S_m}\right) \right)^n \left( \frac{S}{S + K_s \left( 1 - \left(\frac{S}{S_m}\right)^m \right)} \right)$	[15]
Luong	$q_{max} \frac{S}{S + K_s} \left( 1 - \left(\frac{S}{S_m}\right) \right)^n$	[16]
Moser	$\frac{q_{max}S^n}{K_s + S^n}$	[17]
Webb	$\frac{q_{max}S \left( 1 + \frac{S}{K} \right)}{S + K_s + \frac{S^2}{K_i}}$	[18]
Hinshelwood	$q_{max} \frac{S}{K_s + S} (1 - K_p P)$	[19]

Note:

$q_{max}$  maximal specific growth rate  
 $K_s$  half saturation constant  
 $K_i$  inhibition constant  
 $S_m$  maximal concentration of substrate tolerated  
 $K_p$  product inhibition constant  
 $m, n, K$  curve parameters  
 $S$  substrate concentration  
 $p$  product concentration

$$RMSE = \sqrt{\frac{\sum_{i=1}^n (Pd_i - Ob_i)^2}{n-p}} \quad (\text{Eqn. 1})$$

The  $R^2$  value, also known as the coefficient of determination, was used in linear regression to select the model that provided the best fit. On the other hand, in the case of nonlinear regression, the  $R^2$  does not provide a comparative analysis in situations in which the number of parameters in the various models varies. In order to get around this obstacle, the quality of the nonlinear models was determined by adjusting the  $R^2$  value.  $S_y^2$  is the total variance of the y-variable, while RMS stands for residual mean square. These two terms are used in the adjusted  $R^2$  formula (Equations 2 and 3).

$$\text{Adjusted } (R^2) = 1 - \frac{RMS}{S_y^2} \quad (\text{Eqn. 2})$$

$$\text{Adjusted } (R^2) = 1 - \frac{(1-R^2)(n-1)}{(n-p-1)} \quad (\text{Eqn. 3})$$

One can measure the relative quality of various statistical models for a given set of experimental data by using the Akaike Information Criterion (AIC). This criterion was developed by Akaike. Instead, data sets that have a large number of parameters or few values should utilize the AIC that has been corrected, which is denoted by the letter AICc [21]. The AICc was determined using the equation that is presented below (Equation 4).

$$AICc = 2p + n \ln \left( \frac{RSS}{n} \right) + 2(p+1) + \frac{2(p+1)(p+2)}{n-p-2} \quad (\text{Eqn. 4})$$

Another statistical measure that is founded on information theory is known as the Bayesian Information Criterion (BIC) (Equation 5), which can be compared to the AICc. Models with the lowest Bayesian information criterion (BIC) are typically preferred over those with higher BICs when choosing from a finite number of models. It has close ties to the Akaike information criteria and is partially based on the likelihood function (AIC). This error function imposes a harsher penalty on the number of parameters than the AIC does [22].

$$BIC = n \ln \frac{RSS}{n} + p \ln(n) \quad (\text{Eqn. 5})$$

The Hannan–Quinn information criterion, often known as the HQC, is an additional error function approach that is based on the information theory (Equation 7). To evaluate how well a statistical model fits data, experts use the Hannan–Quinn information criterion (HQC). It is a common metric to employ when choosing one model over another. In contrast to the LLF, it is connected to Akaike's information criterion. The HQC, like the AIC, includes a penalty function for the total number of model parameters, however it is significantly bigger than the value assigned by the AIC because the equation contains the  $\ln \ln n$  term [23];

$$HQC = n \times \ln \frac{RSS}{n} + 2 \times p \times \ln(\ln n) \quad (\text{Eqn. 7})$$

Both BF and AF were utilized to evaluate the appropriateness of the models. In order to get a correlation of 1 between the anticipated value and the observed value, the Bias Factor needs to be equal to 1.

The Bias Factor and Accuracy Factor originate from predictive microbiology under the food microbiology field and have found applications in modelling microbial growth that leads to food spoilage [24–31]. A fail-safe model is indicated when the value of the Bias Factor (Equation 8) is greater than 1, and a fail-negative model is indicated when the value of the Bias Factor is less than 1. When compared to 1, a value of Accuracy that is less than 1 indicates a less accurate prediction (Equation 9). One notable disadvantage is their sensitivity to outliers within the dataset. Extreme values can disproportionately impact the calculations, potentially leading to an overemphasis on specific observations that might not be representative of the general trend. Additionally, the interpretation of these factors is context-dependent, lacking a universal threshold for defining acceptable levels of Accuracy or bias. Researchers must carefully consider the specific characteristics of their data and the nature of the curve-fitting task to derive meaningful insights from these factors.

$$\text{Bias factor} = 10 \left( \sum_{i=1}^n \log \frac{(Pd_i/Ob_i)}{n} \right) \quad (\text{Eqn. 8})$$

$$\text{Accuracy factor} = 10 \left( \sum_{i=1}^n \log \frac{|(Pd_i/Ob_i)|}{n} \right) \quad (\text{Eqn. 9})$$

Another parameter-penalized model is MPSD. The Marquardt's percent standard deviation (MPSD). This error function distribution follows the geometric mean error which allows for the penalty to the number of parameters of a model (Equation 10).

$$MPSD = 100 \sqrt{\frac{1}{n-p} \sum_{i=1}^n \left( \frac{Ob_i - Pd_i}{Ob_i} \right)^2} \quad (\text{Eqn. 10})$$

where  $p$  is the number of parameters,  $n$  is the number of experimental data,  $Ob_i$  is the experimental data, and  $Pd_i$  is the value predicted by the model.

However, the Marquardt MPSD approach has certain drawbacks. One notable disadvantage is its sensitivity to the initial parameter values, which can affect the convergence of the Marquardt algorithm. The Accuracy of parameter estimates and the subsequent evaluation of predictive performance through percentage standard deviation may be influenced by the convergence behavior, particularly if the algorithm converges to a local minimum. Additionally, like other metrics involving percentages, the interpretation of MPSD values depends on the scale of the data and may be sensitive to outliers. As with any curve-fitting method, the absence of a universal benchmark for defining an optimal fit complicates the assessment of the absolute goodness of fit without contextual information or comparison to alternative models.

## RESULTS AND DISCUSSION

According to the bacterial growth model analysis, as depicted in **Figs. 1** 9 all of the studied models showed good fittings except Moser, Monod, and Hinshelwood, which showed the poorest curve fitting, while Han-Levenspiel failed to fit the data. The Luong model emerged as the most suitable model, as indicated by its remarkably low values for RMSE, AICc, BIC, MPSD, HQC and modified  $\text{adj}R^2$ . Furthermore, the model's AF and BF values were close to unity (**Table 2**). The experimental data obtained indicates that OPE is toxic and slows down the rate of growth at higher concentrations.

The calculated value for the Luong's constants maximal degradation rate, half saturation constant for maximal degradation, maximal concentration of substrate tolerated and curve parameter that defines the steepness of the growth rate decline from the maximum rate symbolized by  $q_{max}$ ,  $K_s$ ,  $S_m$ , and  $n$  were  $8.91 \text{ h}^{-1}$  (95% confidence interval or C.I. from 7.15 to 10.67), 1116.19 mg/L (95% C.I. from 815.53 to 1416.84), 1074.6 mg/L (95% C.I. from 1037.8 to 1111.5) and 11.90 (95% C.I. from 5.30 to 18.51), respectively.

In practical terms, these biologically meaningful coefficients obtained from the analysis will be highly valuable for guiding and enhancing batch and field experiments. They will allow researchers and environmental scientists to make accurate predictions regarding the growth conditions and needs of the bacterium when employed for the remediation of toxicants in polluted environments. One of the most important parameters in the Luong model is  $S_m$ , which is the maximal concentration of substrate tolerated. The issue of a small number of points in curve-fitting poses as seen in this study forms a significant challenge to the reliability and robustness of the modeling process. One of the primary disadvantages is the limited amount of information available to capture the underlying trends or patterns in the data accurately.

With only a small number of data points, the model may struggle to discern the true nature of the relationship between the variables, leading to potential overfitting or underfitting issues. Overfitting occurs when a model fits the noise in the data rather than the actual pattern, resulting in poor generalization to new data.

On the other hand, underfitting arises when the model is too simplistic to capture the true complexity of the underlying phenomenon. Both scenarios compromise the model's predictive capabilities and hinder its ability to make meaningful extrapolations beyond the observed data points. Additionally, the lack of data points limits the statistical power to detect subtle trends or nonlinear relationships, reducing the overall confidence in the Accuracy and precision of the fitted curve.

Researchers must exercise caution and consider alternative modeling approaches or seek additional data to address the inherent limitations of a few points in curve-fitting endeavors. To date, the majority of the Luong model reported for xenobiotics-degrading bacteria centred on works on phenol-degrading microbial works [32–34] and molybdenum-reducing bacterium [35,36] and no work has been reported for the use of this model in modelling the effect of

**Table 2.** Statistical analysis of the substrate inhibition models utilized in this study.

Model	p	RMSE	adR2	MPSD	AICc	BIC	HQC	BF	AF
Luong	4	0.012	1.000	1.37	10.42	-59.80	-62.26	1.00	1.00
Yano	4	0.361	0.862	12.19	57.79	-12.42	-14.88	1.01	1.06
Tessier-Edward	3	0.493	0.743	19.63	20.17	-7.99	-9.83	1.04	1.13
Aiba	3	0.427	0.806	18.21	18.17	-10.00	-11.84	1.05	1.12
Haldane	3	0.398	0.840	14.80	17.18	-10.99	-12.83	1.03	1.09
Monod	2	0.477	0.772	19.12	5.29	-8.82	-10.05	1.05	1.14
Han and Levenspiel	5	n.a.	n.a.	n.a.	n.a.	n.a.	n.a.	n.a.	n.a.
Moser	3	0.464	0.797	20.98	19.33	-8.83	-10.67	0.98	1.12
Hinshelwood	4	0.616	0.545	24.68	65.29	-4.93	-7.38	1.05	1.14
Webb	4	0.459	0.760	17.09	61.18	-9.04	-11.50	1.03	1.09

Note:  $p$  is the number of parameters

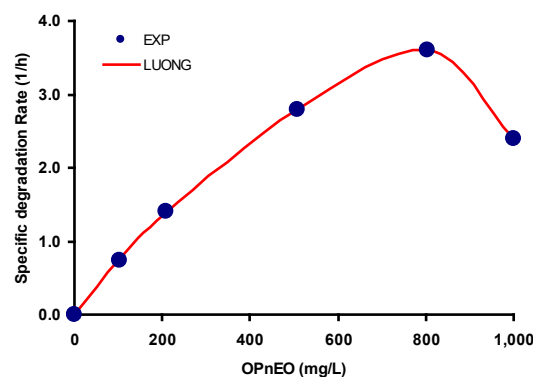


**Fig. 1.** Growth of *Aeromonas* sp. TXBc10 modeled using Luong.

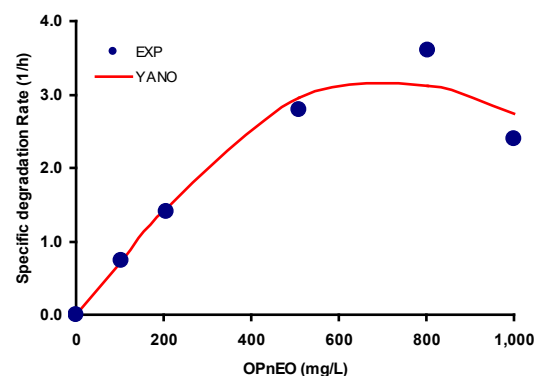


**Fig. 2.** Growth of *Aeromonas* sp. TXBc10 modeled using Yano.

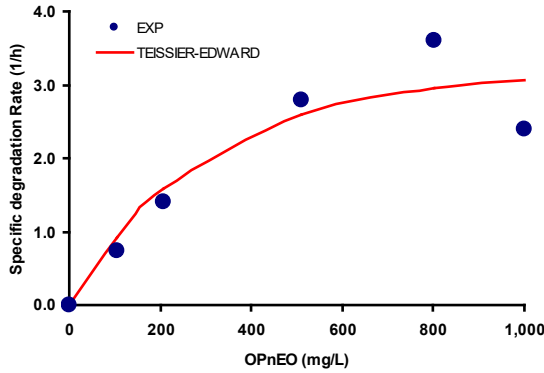


Fig. 3. Growth of *Aeromonas* sp. TXBc10 modeled using Teissier-Edward.

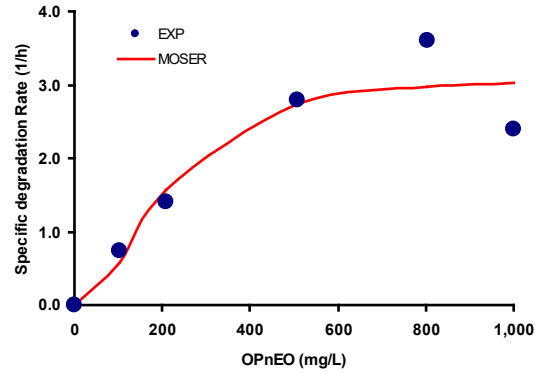


Fig. 7. Growth of *Aeromonas* sp. TXBc10 modeled using Moser.

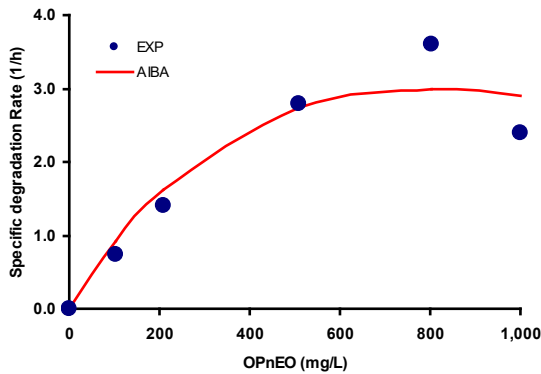


Fig. 4. Growth of *Aeromonas* sp. TXBc10 modeled using Aiba.

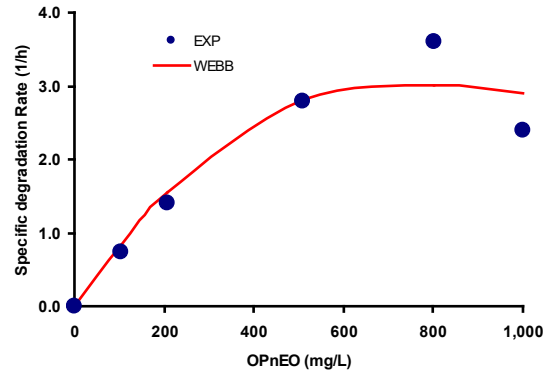


Fig. 8. Growth of *Aeromonas* sp. TXBc10 modeled using Webb.

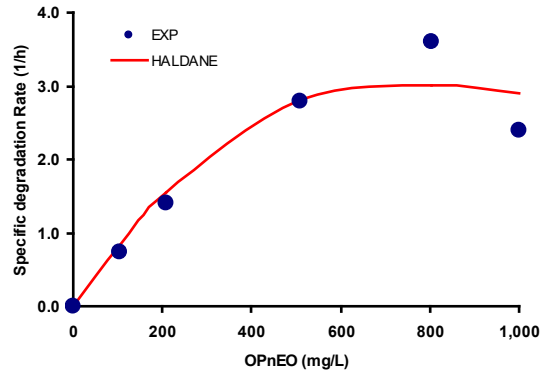


Fig. 5. Growth of *Aeromonas* sp. TXBc10 modeled using Haldane.

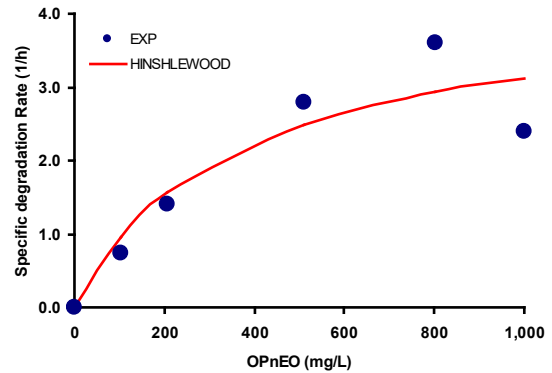


Fig. 9. Growth of *Aeromonas* sp. TXBc10 modeled using Hinshelwood.

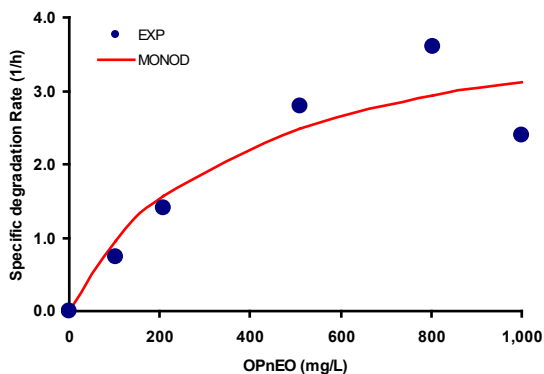


Fig. 6. Growth of *Aeromonas* sp. TXBc10 modeled using Monod.

The biologically significant coefficients obtained from this analysis have practical implications, offering valuable guidance for optimizing both batch and field experiments. These coefficients serve as a crucial tool for researchers and environmental scientists, facilitating precise predictions regarding *Aeromonas* sp's growth conditions and requirements. TXBc10. This information is particularly relevant in the context of remediating Octylphenol Polyethoxylates (OPE) in polluted environments.

The utilization of a substrate inhibition kinetics model is increasingly recognized as a pivotal approach for assessing the impact of toxic compounds on microbial growth or degradation rates (Table 3). Traditionally, many studies have favored the Haldane or Monod models for modeling purposes.



However, a select few, including this study, opt for a comprehensive modeling approach, capitalizing on the flexibility offered by alternative models. This inclusive strategy improves curve fitting results compared to popular models and represents a nuanced and thorough methodology for comprehending the intricate dynamics of microbial responses to toxic compounds. In the specific case of *Aeromonas* sp. TXBc10, the application of substrate inhibition kinetics provides a more detailed understanding of its behavior in OPE remediation, contributing to the broader field of environmental microbiology.

**Table 3.** Characteristics of various microorganisms involved in the degradation of octylphenol polyethoxylates and related compounds.

Microorganism	Optimum pH	Optimum Temperature °C	Primary Growth Models (e.g., Modified Gompertz)	Secondary Substrate Inhibition Kinetics	Type of Compound Studied	Ref
<i>Aeromonas</i> sp. TXBc10	8.0	30	No	No	Octylphenol Polyethoxylates	[3]
<i>Brevibacterium</i> sp. TX4	7.5	28	No	No	Octylphenol Polyethoxylates	[37]
Soil Bacteria	7.0	30	No	No	Octylphenol Polyethoxylates	[38]
<i>Pseudomonas nitroreducens</i> TX1	7.2	25	No	No	Octylphenol Polyethoxylates	[39]
<i>Pseudomonas nitroreducens</i> TX1	n.a.	n.a.	No	Teissier	Octylphenol Polyethoxylates	[40] (remodel)
<i>Pseudomonas</i> sp. SH4	7.0	30	No	No	Octylphenol Polyethoxylates	[41]
Nonylphenol-Degrading Bacteria	7.5	30	No	No	Nonylphenol Polyethoxylates	[42]
<i>Sphingomonas</i> sp. Y2	7.2		Modified Gompertz	No	Nonylphenol Polyethoxylate	[43]
<i>Aeromonas</i> sp. TXBc10			No	Luong	Octylphenol Polyethoxylates	This study (remodel)

## CONCLUSION

In conclusion, after conducting a comprehensive analysis that included various statistical metrics such as the corrected AICc (Akaike Information Criterion), bias factor (BF), adjusted coefficient of determination ( $R^2$ ), and root-mean-square error (RMSE), it has been determined that the Luong model stands out as the most suitable model for describing the growth of the bacterium on OPE. This model's superiority was clearly evident through these statistical assessments. From the fitting exercise, we were able to extract valuable parameters for the model. The Luong model allows an important parameter to be obtained that is the maximum concentration of substrate that causes complete cessation of degradation rate. This knowledge will be instrumental in designing effective strategies for addressing environmental contamination and further advancing our understanding of microbial processes in environmental remediation.

## REFERENCES

- Osimitz TG, Droege W, Driver JH. Human Risk Assessment for Nonylphenol. *Hum Ecol Risk Assess Int J*. 2015 Oct 3;21(7):1903–19.

- Schüürmann G. Acute aquatic toxicity of alkyl phenol ethoxylates. *Ecotoxicol Environ Saf*. 1991 Apr 1;21(2):227–33.
- Yan B, Luo L, Yang H. Isolation and characterization of *Aeromonas* sp. TXBc10 capable of high-efficiency degradation of octylphenol polyethoxylate from tannery wastewater. *Environ Technol*. 2020 Dec 18;41(28):3722–31.
- Baldwin WS, Graham SE, Shea D, LeBlanc GA. Altered Metabolic Elimination of Testosterone and Associated Toxicity Following Exposure of *Daphnia magna* to Nonylphenol Polyethoxylate. *Ecotoxicol Environ Saf*. 1998 Feb 1;39(2):104–11.
- TenEyck MC, Markee TP. Toxicity of Nonylphenol, Nonylphenol Monoethoxylate, and Nonylphenol Diethoxylate and Mixtures of these Compounds to *Pimephales promelas* (Fathead Minnow) and *Ceriodaphnia dubia*. *Arch Environ Contam Toxicol*. 2007 Nov 1;53(4):599–606.
- Song M, Bielefeldt AngelaR. Toxicity and inhibition of bacterial growth by series of alkylphenol polyethoxylate nonionic surfactants. *J Hazard Mater*. 2012 Jun 15;219–220:127–32.
- Rohatgi A. WebPlotDigitizer User Manual 4.3. [Http://rohatgi.info/WebPlotDigitizerapp](http://rohatgi.info/WebPlotDigitizerapp) Accessed June 2 2014. 2020;1–17.
- Yahuza S, Dan-iyi BI, Sabo IA. Modelling the Growth of *Enterobacter* sp. on Polyethylene. *J Biochem Microbiol Biotechnol*. 2020;8(1):42–6.
- Sabo IA, Yahuza S, Shukor MY. Molybdenum Blue Production from *Serratia* sp. strain DRY5: Secondary Modeling. *Bioremediation Sci Technol Res*. 2021;9(2):21–4.
- Monod J. The Growth of Bacterial Cultures. *Annu Rev Microbiol*. 1949;3(1):371–94.
- Boon B, Laudelout H. Kinetics of nitrite oxidation by *Nitrobacter winogradskyi*. *Biochem J*. 1962;85:440–7.
- Teissier G. Growth of bacterial populations and the available substrate concentration. *Rev Sci Instrum*. 1942;3208:209–14.
- Aiba S, Shoda M, Nagatani M. Kinetics of product inhibition in alcohol fermentation. *Biotechnol Bioeng*. 1968 Nov 1;10(6):845–64.
- Yano T, Koga S. Dynamic behavior of the chemostat subject to substrate inhibition. *Biotechnol Bioeng*. 1969 Mar 1;11(2):139–53.
- Han K, Levenspiel O. Extended Monod kinetics for substrate, product, and cell inhibition. *Biotechnol Bioeng*. 1988;32(4):430–7.
- Luong JHT. Generalization of monod kinetics for analysis of growth data with substrate inhibition. *Biotechnol Bioeng*. 1987;29(2):242–8.
- Moser A. Kinetics of batch fermentations. In: Rehm HJ, Reed G, editors. *Biotechnology*. VCH Verlagsgesellschaft mbH, Weinheim; 1985. p. 243–83.
- Webb J. *Enzyme and metabolic inhibitors* [Internet]. New York: Academic Press; 1963. 984 p. Available from: <https://www.biodiversitylibrary.org/bibliography/7320>
- Hinshelwood CN. *The chemical kinetics of the bacterial cell*. Clarendon Press, Gloucestershire, UK; 1946.
- Wayman M, Tseng MC. Inhibition-threshold substrate concentrations. *Biotechnol Bioeng*. 1976;18(3):383–7.
- Akaike H. Making statistical thinking more productive. *Ann Inst Stat Math*. 2010;62(1):3–9.
- Kass RE, Raftery AE. Bayes Factors. *J Am Stat Assoc*. 1995 Jun 1;90(430):773–95.
- Burnham KP, Anderson DR. *Model Selection and Multimodel Inference: A Practical Information-Theoretic Approach*. Springer Science & Business Media; 2002. 528 p.
- Ross T, McMeekin TA. Predictive microbiology. *Int J Food Microbiol*. 1994;23(3–4):241–64.
- Zhou K, George SM, Métris A, Li PL, Baranyi J. Lag phase of *Salmonella enterica* under osmotic stress conditions. *Appl Environ Microbiol*. 2011;77(5):1758–62.
- Zhao J, Gao J, Chen F, Ren F, Dai R, Liu Y, et al. Modeling and predicting the effect of temperature on the growth of *Proteus mirabilis* in chicken. *J Microbiol Methods*. 2014;99(1):38–43.
- Velugoti PR, Bohra LK, Juneja VK, Huang L, Wesseling AL, Subbiah J, et al. Dynamic model for predicting growth of *Salmonella* spp. in ground sterile pork. *Food Microbiol*. 2011;28(4):796–803.
- McElroy DM, Jaykus LA, Foegeding PM. Validation and analysis of modeled predictions of growth of *Bacillus cereus* spores in boiled rice. *J Food Prot*. 2000;63(2):268–72.

29. Kowalik J, Lobacz A, Tarczynska AS, Ziajka S. Graphie validation of growth models for *Listeria monocytogenes* in milk during storage. *Milchwissenschaft*. 2012;67(1):38–42.
30. Jung SH, Park SJ, Chun HH, Song KB. Effects of combined treatment of aqueous chlorine dioxide and fumaric acid on the microbial growth in fresh-cut paprika (*capsicum annum* L.). *J Appl Biol Chem*. 2014;57(1):83–7.
31. Huang L, Hwang CA, Phillips J. Evaluating the Effect of Temperature on Microbial Growth Rate-The Ratkowsky and a B  lehr  dek-Type Models. *J Food Sci*. 2011;76(8):M547–57.
32. Hamitouche AE, Bendjama Z, Amrane A, Kaouah F, Hamane D. Relevance of the Luong model to describe the biodegradation of phenol by mixed culture in a batch reactor. *Ann Microbiol*. 2012;62(2):581–6.
33. Halmi MIE, Shukor MS, Johari WLW, Shukor MY. Mathematical modelling of the degradation kinetics of *Bacillus cereus* grown on phenol. *J Environ Bioremediation Toxicol*. 2014;2(1):1–5.
34. Hasan SA, Jabeen S. Degradation kinetics and pathway of phenol by *Pseudomonas* and *Bacillus* species. *Biotechnol Biotechnol Equip*. 2015 Jan 2;29(1):45–53.
35. Othman AR, Bakar NA, Halmi MIE, Johari WLW, Ahmad SA, Jirangon H, et al. Kinetics of molybdenum reduction to molybdenum blue by *Bacillus* sp. strain A.rzi. *BioMed Res Int*. 2013;2013:Article number 371058.
36. Shukor MS, Shukor MY. Statistical diagnostic tests of the Luong model in fitting molybdenum reduction from the bacterium *Bacillus* sp. strain A.rzi. *J Environ Microbiol Toxicol*. 2014;2(2):53–7.
37. Lin YW, Yang CC, Tuan NN, Huang SL. Diversity of octylphenol polyethoxylate-degrading bacteria: With a special reference to *Brevibacterium* sp. TX4. *Int Biodeterior Biodegrad*. 2016 Nov 1;115:55–63.
38. Rulianti AD, Hasegawa M, Ikunaga Y, Sato Y, Ohta H. Isolation of Octylphenol Polyethoxylate-Degrading Soil Bacteria: a Long-Term Soil Column Study. *Microbes Environ*. 2007;22(4):391–8.
39. Chen HJ, Guo GL, Tseng DH, Cheng CL, Huang SL. Growth factors, kinetics and biodegradation mechanism associated with *Pseudomonas nitroreducens* TX1 grown on octylphenol polyethoxylates. *J Environ Manage*. 2006 Sep 1;80(4):279–86.
40. Abubakar A, Yakasai HM, Uba G, Sabo I. Substrate Inhibition Modelling of *Pseudomonas nitroreducens* Growth on Octylphenol Polyethoxylates. *J Environ Microbiol Toxicol*. 2023 Jun 30;11(1):25–31.
41. Chen HJ, Huang SL, Tseng DH. Aerobic biotransformation of octylphenol polyethoxylate surfactant in soil microcosms. *Environ Technol*. 2004 Feb 1;25(2):201–10.
42. Maeda T, Hayakawa K, You M, Sasaki M, Yamaji Y, Furushita M, et al. Characteristics of Nonylphenol Polyethoxylate-Degrading Bacteria Isolated from Coastal Sediments. *Microbes Environ*. 2005;20(4):253–7.
43. Bai N, Wang S, Abuduaini R, Zhu X, Zhao Y. Isolation and characterization of *Sphingomonas* sp. Y2 capable of high-efficiency degradation of nonylphenol polyethoxylates in wastewater. *Environ Sci Pollut Res*. 2016 Jun 1;23(12):12019–29.